Geochemical Perspectives Letters

Experimental clues for detecting biosignatures on Mars

J.-C. Viennet[1,2*], S. Bernard[1], C. Le Guillou[3], P. Jacquemot[1,2], E. Balan[1], L. Delbes[1], B. Rigaud[4], T. Georgelin[5], M. Jaber[2]

doi: 10.7185/geochemlet.1931

Abstract

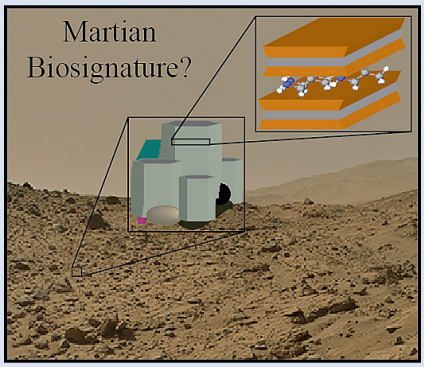

Forthcoming exploration of Mars aims at identifying fossil biosignatures within ancient clay-rich formations. The subsurface of Mars has mostly acted as a giant freezer for the last 4 Gyr, thereby preserving potential remains of martian life. Yet, volcanism and impactors have periodically triggered the circulation of hydrothermal fluids, inevitably causing alteration of potentially fossilised biogenic organic materials. It thus appears crucial to quantify the impact of hydrothermal processes on organic biogeochemical signals in the presence of clay minerals. Here, we submitted RNA to hydrothermal conditions in the presence of Mg-smectites. Results show heterogeneous organo-mineral residues, with sub-micrometric phosphates, carbonates and amorphous silica particles together with Mg-smectites with interlayer spaces saturated by N-rich organic compounds. Although the chemical structure of RNA did not withstand hydrothermal conditions, clay minerals efficiently trapped organic carbon, confirming the relevance of drilling for organic carbon in ancient martian sediments. In addition, the degradation of RNA in the presence of Mg-smectites led to the precipitation of a quite uncommon mineral assemblage that could be seen as a biosignature *per se*. Martian targets exhibiting this mineral assemblage will thus constitute high priority and highly relevant candidates for sample return.

Received 25 February 2019 | Accepted 7 November 2019 | Published 27 November 2019

Letter

Life may have existed on Mars. In fact, some evidence suggest that conditions were favourable for life to exist on Mars during the Noachian (~4.1 to 3.7 Ga), from both the standpoints of liquid water availability and metabolic energy sources (Grotzinger *et al.*, 2014; Kral *et al.*, 2014). Following previous successful missions that visited the red planet, upcoming exploration of Mars aims at identifying potential fossilised biosignatures (Mustard *et al.*, 2013; Westall *et al.*, 2015; Vago *et al.*, 2017), with organic carbon obviously constituting the grail to be sought after (Summons *et al.*, 2008; McMahon *et al.*, 2018). To date, although macromolecular carbon has been detected within most of the martian meteorites (Steele *et al.*, 2016, 2018), only small organic molecules including aromatic, aliphatic, chlorine- and sulfur-rich organic compounds have been measured on Mars (Biemann *et al.*, 1977; Freissinet *et al.*, 2015; Eigenbrode *et al.*, 2018).

Because of the lack of global plate tectonic processes, traces of this life could be preserved in martian sedimentary rocks despite the continuous UV irradiation of the surface (Cockell, 2002). In fact, the subsurface of Mars has acted as a giant freezer since the Noachian (3.7 Ga) (Clifford *et al.*, 2010). However, even if the surface of Mars has been relatively inactive compared to Earth, volcanism and impactors have periodically triggered the circulation of hydrothermal fluids, inevitably causing alteration of potentially fossilised biogenic organic materials (Abramov and Kring, 2005; Schwenzer and Kring, 2009; Osinski *et al.*, 2013).

In the context of the massive international push for the astrobiological exploration of Mars, the forthcoming ExoMars and Mars2020 missions will explore the subsurface of ancient (>3.7 Ga) clay-rich martian terrains that likely formed in the presence of water (Ehlmann *et al.*, 2008; Mustard *et al.*, 2013; Westall *et al.*, 2015; Vago *et al.*, 2017). Clay minerals, and smectites in particular, are the prime target of these missions because of their strong absorption capacity, low reactivity, and low permeability when compacted (Kennedy *et al.*, 2002; Naimark *et al.*, 2016; McMahon *et al.*, 2018), giving them a high 'potential of biopreservation'. The presence of these minerals at landing sites is thus believed to maximise the chances of detecting diagnostic organic molecules.

1. Muséum National d'Histoire Naturelle, Sorbonne Université, CNRS, UMR 7590, Institut de Minéralogie, Physique des Matériaux et Cosmochimie, Paris, France
2. Laboratoire d'Archéologie Moléculaire et Structurale, CNRS UMR 8220, Institut des Matériaux de Paris, Sorbonne Université, F-75005 Paris, France
3. Université de Lille, CNRS, INRA, ENSCL, UMR 8207 - UMET - Unité Matériaux et Transformations, F-59000 Lille, France
4. Institut des Matériaux de Paris Centre, Sorbonne Université, F-75005 Paris, France
5. Laboratoire de Réactivité de Surface, CNRS, UMR 7197, Institut des Matériaux de Paris, Sorbonne Université, F-75005 Paris, France
* Corresponding author (email: jean.christophe.viennet25@gmail.com)

Nevertheless, little is known regarding the interactions between clay minerals and (biogenic or abiotic) organic compounds under hydrothermal conditions that may have existed in the subsurface of Mars. Better constraining the impact of hydrothermal processes on fossilised organic biosignatures thus appears fundamental in conducting the future search for traces of life on Mars with any reasonable degree of confidence. Only laboratory experiments can provide the necessary insights.

RNA is the most emblematic biogenic organic molecule used by all known living organisms, and potentially the most ancient replicating molecule on Earth according to the 'RNA world' hypothesis (Higgs and Lehman, 2014). Mg-smectites are one of the most widespread clay minerals present on Mars and on the future landing sites (Ehlmann *et al.*, 2008; Vago *et al.*, 2017). Here, we heated RNA at hydrothermal conditions in pure bi-distilled water in equilibrium with a CO_2 atmosphere at 200 °C for 7 days in the presence of Mg-smectites. We conducted additional experiments under the same conditions with RNA in the absence of Mg-smectites and with Mg-smectites in the absence of RNA to serve as controls. A CO_2 atmosphere was used to simulate Noachian martian atmosphere (Wordsworth, 2016). The water insoluble experimental residues were characterised at different scales using X-ray diffraction and advanced microscopy and spectroscopy tools.

Results show that the presence of Mg-smectites considerably impacts the amount of carbon and nitrogen retrieved in the residues after the experiments. While only 7.8 wt. % of the initial carbon and 1.7 wt. % of the initial nitrogen are found in the organic residues of experiments conducted in the absence of smectite, 36.5 wt. % of the initial carbon and 10.8 wt. % of the initial nitrogen remain in the organo-mineral residues of the experiments conducted with Mg-smectites. These amounts correspond to a mean N/C of 0.11 for the organic component and to TOC values as high as 6.5 wt. % (Table 1), *i.e.* twice the values of most of the hydrocarbon source rocks on Earth (Bernard and Horsfield, 2014). As expected, the presence of clay minerals thus drastically maximises the chances of concentrating, preserving, and ultimately detecting organic molecules.

Table 1 Proportions of carbon and nitrogen (in mass).

Sample	RNA	Mg-smectites-RNA-CO_2-200 °C	RNA-CO_2-200 °C
Initial mass of organic matter (mg)	-	150	150
Final mass of sample (mg)	-	270	7.0
$\%_{wt}$ C	31.6 (±0.07)	6.4 (±0.07)	52.9 (±0.07)
Initial mass of C (mg)		47.4	47.4
Final mass of C (mg)	-	17.3	3.7
% of C preserved		36.5	7.8
$\%_{wt}$ N	14.9 (±0.02)	0.9 (±0.02)	5.7 (±0.02)
Initial mass of N (mg)		22.3	22.3
Final mass of N (mg)	-	2.4	0.4
% of N preserved		10.8	1.7

Surprisingly, even though the present experiments were conducted using pure Mg-smectites and pure RNA, the organo-mineral residues are highly heterogeneous. In addition to Mg-smectites, transmission electron microscopy investigations in STEM mode (scanning transmission electron microscopy) highlight the presence of Ca-carbonates and Mg, Ca and Al-phosphates, together with particles of amorphous silica (Fig. 1). This occurrence of phosphates is attested by diagnostic peaks observed in the XRD pattern (Fig. 2) and the presence of carbonates is confirmed by diagnostic features in the XANES and MIR spectra (Figs. 1 and 2).

The organic carbon of the residues appears essentially coupled with Mg-smectites and exhibits a XANES spectrum very different from that of RNA (Fig. 1). The XANES spectrum of RNA presents a series of peaks attributed to nucleobases (aromatic and olefinic carbons (285 eV), heterocycles (285.9 eV), ketone and phenol groups (286.7 - 287.4 eV)) and ribose (saturated carbons (288.0 eV) and hydroxyl groups (289.3 eV)). In contrast, the organic compounds coupled with smectites in the experimental residues mainly contain amide (288.2 eV) and saturated aliphatic (288.0 eV) groups, as well as aromatic and/or olefinic carbons (285 eV) and ketone and/or phenol groups (287.4 eV). Occurrence of saturated aliphatic groups is also attested by diagnostic C-H stretching bands observed in the ATR-FTIR spectrum (Fig. 2).

In addition to the compounds found with smectites (N/C = 0.11), the experimental residues also contain some rare organic masses (N/C = 0.15) whose spectra display peaks of aromatic and olefinic carbons (285 eV), conjugated (hetero) cycles (285.4 eV) and carboxylic groups (288.4 eV), as well as some even rarer aromatic particles (N/C < 0.05) whose spectra only display peaks of aromatic and olefinic carbons (285 eV) and conjugated (hetero)cycles (285.4 eV) (Fig. 1) (Le Guillou *et al.*, 2018). These compounds are not present in high concentrations, the organic component of the residues essentially consisting of the compounds associated with Mg-smectites, explaining bulk N/C values.

The crystal structure of the Mg-smectites does not suffer significant transformation during the experiments (same hkl reflections on the XRD pattern and similar IR bands related to Mg-OH or Si-O vibrations; Fig. 2). However, the 001 reflection is shifted from 15.51 to 13.31 Å (Fig. 2), indicating a modification of the interlayer spaces. The observed shift is consistent with the presence of organic molecules and/or a mixture of bi- and mono-hydrated cations in the interlayer space (Ferrage *et al.*, 2005; Gautier *et al.*, 2017). Bands at ~1440 and ~1580 cm^{-1} in the FTIR spectrum of experimental residues are consistent with the presence of NH_4^+ and R-NH_3^+ groups, respectively.

The presence of ammonium in the interlayer spaces of smectites is excluded, however. In fact, for those exposed to high vacuum, the 001 reflections of the experimental residues and of the pristine Mg-smectites saturated with NH_4^+ exhibit a markedly different behaviour (Fig. 2), showing that the interlayer spaces of these smectites are locked by N-rich organic compounds rather than by ammonium. Consistently with XANES data indicating N/C values of 0.11 for these compounds, XRD data show a 001 reflection at 13.55 Å for the Mg-smectites of the residues (Fig. 2) indicating the presence, within the interlayer spaces, of organic compounds containing up to 10 carbon atoms for 1 R-NH_3^+ group (*i.e.* N/C values of about 0.1) according to the alkylammonium method (Laird *et al.*, 1989). Assuming that R-NH_3^+ groups totally compensate the loss of Ca^{2+}, the Mg-smectites contain 1.3 wt. % of nitrogen, and thus 10.9 wt. % of carbon (N/C = 0.1). Given that the residues exhibit a TOC of 6.5 wt. %, assuming that most of the organic compounds of the experimental residues are within the interlayer spaces of the Mg-smectites leads to a proportion of approximately 60 wt. % of Mg-smectites in the residues, which is quite consistent with TEM data.

The formation of the observed mineral assemblage can be explained as follows (Fig. 3). Under hydrothermal conditions, the dissolution of the Mg-smectites, together with the

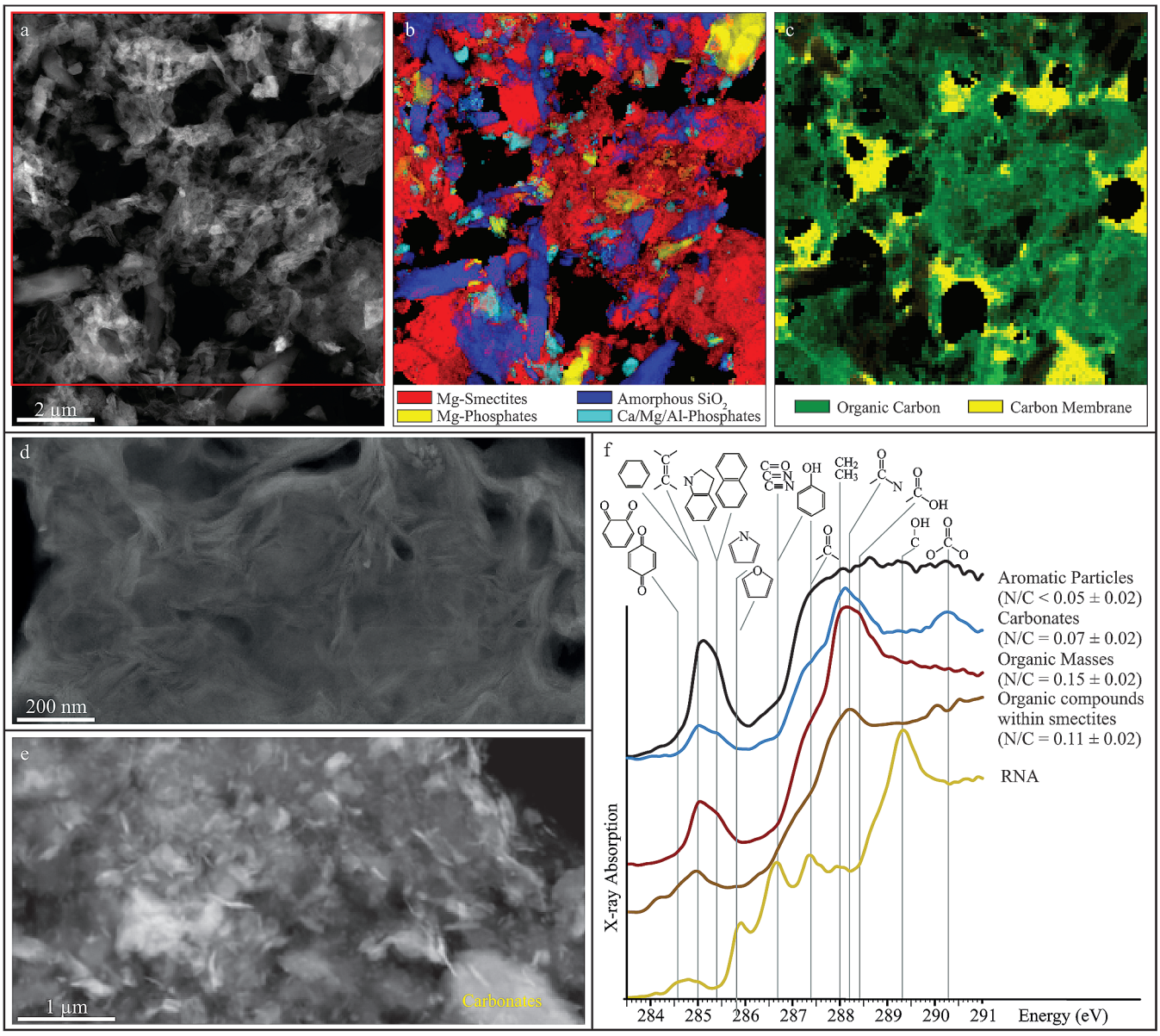

Figure 1 STEM and STXM characterisation of the experimental residues. **(a)** STEM image of the residues of experiments conducted under CO_2 at 200 °C in the presence of Mg-smectites and RNA. **(b,c)** Maps of minerals and organic compounds (same area as **a**). **(d)** STEM images of Mg-smectites. **(e)** STEM image of sub-micrometric minerals embedded in organic masses. **(f)** XANES spectra of organic compounds encountered in the residues. The spectrum of RNA is shown for comparison.

interlayer cationic exchange, releases Al, Mg and Ca in the system. Ca-carbonates then precipitate, the carbon source being either RNA degradation products (Sagemann *et al.*, 1999) or the CO_2 rich atmosphere (Viennet *et al.*, 2017, 2019). Meanwhile, the phosphate mono-ester groups of RNA underwent hydrolysis, leading to the precipitation of Al, Ca and Mg-phosphates (Fig. 3; Saxby, 2012). Amorphous SiO_2 particles were formed, as in dissolution experiments (Robin *et al.*, 2016). In parallel, the N-rich aliphatic organic compounds produced by the degradation of RNA are trapped mainly in the interlayer spaces of the remaining Mg-smectites as a result of cationic exchange (Fig. 3). The NH_3^+ groups of these organic compounds replace the initial Ca^{2+} cations in the interlayer spaces of the Mg-smectites (Laird *et al.*, 1989).

Taken altogether, the results of the present experiments are of major importance for the upcoming astrobiological exploration of Mars. Although the organic compounds present in the residues do not carry any information on the chemical structure of the organic starting material, these experimental results demonstrate that clay minerals can efficiently trap organic carbon under hydrothermal conditions, providing strong support for the strategy of drilling for organic carbon in martian subsurface (Eigenbrode *et al.*, 2018; McMahon *et al.*, 2018).

As shown here, the hydrothermal degradation of (N, P)-rich organic molecules in the presence of Mg-smectites leads to the precipitation of a quite uncommon mineral assemblage comprising sub-micrometric Ca-carbonates and (Al, Mg, Ca)-phosphates, together with amorphous silica and clay-organic complexes. Such an assemblage will be stable under martian subsurface conditions for eons. Martian targets exhibiting this mineral assemblage will thus constitute high priority and highly relevant candidates for sample return because of the likelihood that they result from the hydrothermal degradation of (N, P)-rich biogenic organic molecules. As a corollary, the presence and the nature of organic materials within martian rocks should not be the only 'biosignatures' to consider when searching for traces of life: the nature of the mineral assemblage may be even richer in information.

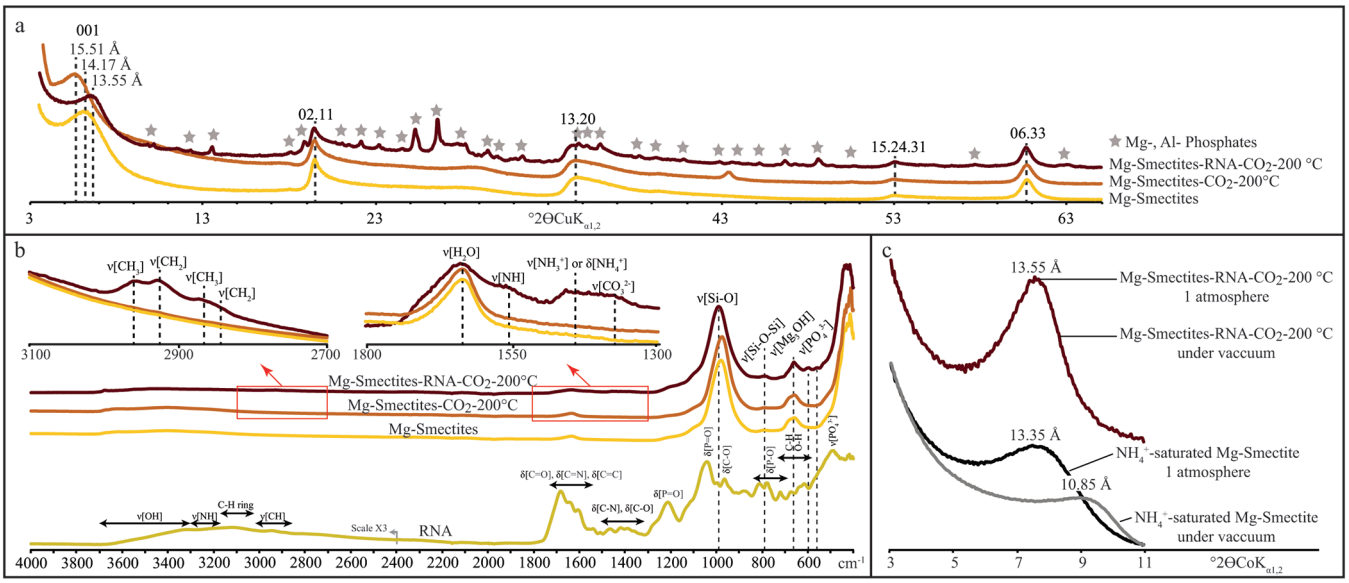

Figure 2 XRD and Mid-IR characterisation of the residues of experiments conducted under CO_2 at 200 °C in the presence or absence of RNA. **(a)** Powder XRD patterns of the synthetic Mg-smectites and of the experimental residues. Values correspond to hkl reflections of the Mg-smectites. **(b)** Mid-infrared ATR spectra of the starting materials (RNA and Mg-smectites) and of the residues. **(c)** XRD patterns at 1 atmosphere and under vacuum of the pristine Mg-smectites saturated with NH_4^+ and of the residues. Values correspond to the 001 reflection.

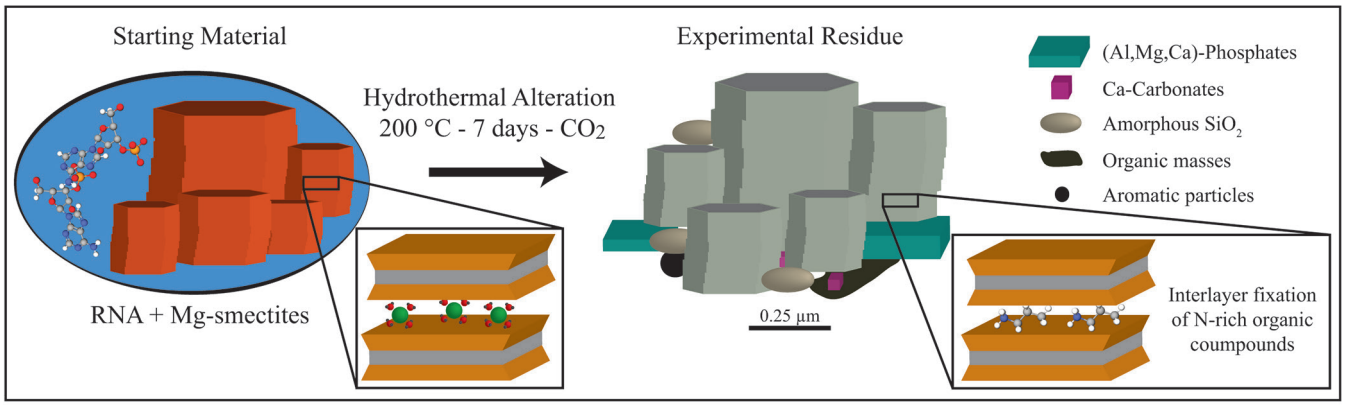

Figure 3 Schematic representation of the results of the present experiments.

In summary, the pilot experiments reported here provide new leads for the (indirect) detection of (biogenic) organic carbon in the martian subsurface. Extrapolating laboratory results to geological timescales is not straightforward (Alleon *et al.*, 2017). Achieving a mechanistic understanding of biosignature taphonomy processes on Mars will require many additional experimental studies.

In addition to offering new perspectives for the search for traces of life on Mars, the present study also provides a strong rationale for the search for potential biosignatures on other planetary bodies, including rocky and/or icy ones (such as Ceres, Enceladus or Europa) on which hydrothermal systems and/or N-rich clay minerals have recently been detected (Carrozzo *et al.*, 2018; Nordheim *et al.*, 2018; Marchi *et al.*, 2019). As illustrated here, laboratory experiments are key steps to support astrobiological exploration seeking to provide evidence of the existence of extraterrestrial life.

Acknowledgements

The authors wish to acknowledge the workforce of the spectroscopic and X-ray diffraction facilities at IMPMC. Special thanks go to Stefan Stanescu and Sufal Swaraj for their expert support with the HERMES STXM beamline at SOLEIL, to Anne-Marie Blanchenet for her help during the Cryo-ultramicrotome section preparations and to François Baudin for his help with CHNS measurements. We gratefully acknowledge financial support from the programme Emergences Sorbonne Universités (Project MarsAtLab - PI: S. Bernard) and the DIM MAP (Project FossilEx - PI: M. Jaber). The authors thank also Dr. Roger Hewins for polishing the English. The TEM facility in Lille (France) is supported by the Conseil Régional du Nord-Pas de Calais, and the European Regional Development Fund (ERDF). The HERMES beamline (SOLEIL) is supported by the CNRS, the CEA, the Region Ile de France, the Departmental Council of Essonne and the Region Centre. The authors wish to acknowledge the Editor Pr. Liane G. Benning, as well as two anonymous reviewers, for their constructive comments that greatly improved the quality of this work.

Editor: Liane G. Benning

Author Contributions

JCV, SB and MJ designed the present study. JCV conducted the hydrothermal experiments. JCV performed CHNS

measurements. JCV, CLG and PJ performed STEM analyses. JCV, SB and CLG performed STXM-XANES analyses. JCV and EB performed IR analyses. JCV and LD performed XRD analyses. All authors contributed to the interpretation of the results. JCV and SB wrote the manuscript, with critical inputs from CLG, EB and MJ.

Additional Information

Supplementary Information accompanies this letter at http://www.geochemicalperspectivesletters.org/article1931.

Cite this letter as: Viennet, J.-C., Bernard, S., Le Guillou, C., Jacquemot, P., Balan, E., Delbes, L., Rigaud, B., Georgelin, T., Jaber, M. (2019) Experimental clues for detecting biosignatures on Mars. *Geochem. Persp. Let.* 12, 28–33.

References

Abramov, O., Kring, D.A. (2005) Impact-induced hydrothermal activity on early Mars. *Journal of Geophysical Research: Planets* 110.

Alleon, J., Bernard, S., Le Guillou, C., Daval, D., Skouri-Panet, F., Kuga, M., Robert, F. (2017) Organic molecular heterogeneities can withstand diagenesis. *Scientific Reports* 7, 1508.

Bernard, S., Horsfield, B. (2014) Thermal Maturation of Gas Shale Systems. *Annual Review of Earth and Planetary Sciences* 42, 635–651.

Biemann, K., Oro, J., Toulmin, P., Orgel, L.E., Nier, A.O., Anderson, D.M., Simmonds, P.G., Flory, D., Diaz, A. V, Rushneck, D.R., Biller, J.E., Lafleur, A.L. (1977) The search for organic substances and inorganic volatile compounds in the surface of Mars. *Journal of Geophysical Research* 82, 4641–4658.

Carrozzo, F.G., De Sanctis, M.C., Raponi, A., Ammannito, E., Castillo-Rogez, J., Ehlmann, B.L., Marchi, S., Stein, N., Ciarniello, M., Tosi, F., Capaccioni, F., Capria, M.T., Fonte, S., Formisano, M., Frigeri, A., Giardino, M., Longobardo, A., Magni, G., Palomba, E., Zambon, F., Raymond, C.A., Russell, C.T. (2018) Nature, formation, and distribution of carbonates on Ceres. *Science Advances* 4, e1701645.

Clifford, S.M., Lasue, J., Heggy, E., Boisson, J., McGovern, P., Max, M.D. (2010) Depth of the Martian cryosphere: Revised estimates and implications for the existence and detection of subpermafrost groundwater. *Journal of Geophysical Research: Planets* 115.

Cockell, C.S. (2002) The Ultraviolet Radiation Environment of Earth and Mars: Past and Present. In: Horneck, G., Baumstark-Khan, C. (Eds.) *Astrobiology: The Quest for the Conditions of Life*. Springer Berlin Heidelberg, Berlin, Heidelberg, 219–232.

Ehlmann, B.L., Mustard, J.F., Fassett, C.I., Schon, S.C., Head III, J.W., Des Marais, D.J., Grant, J.A., Murchie, S.L. (2008) Clay minerals in delta deposits and organic preservation potential on Mars. *Nature Geoscience* 1, 355.

Eigenbrode, J.L., Summons, R.E., Steele, A., Freissinet, C., Millan, M., Navarro-González, R., Sutter, B., McAdam, A.C., Franz, H.B., Glavin, D.P., Archer, P.D., Mahaffy, P.R., Conrad, P.G., Hurowitz, J.A., Grotzinger, J.P., Gupta, S., Ming, D.W., Sumner, D.Y., Szopa, C., Malespin, C., Buch, A., Coll, P. (2018) Organic matter preserved in 3-billion-year-old mudstones at Gale crater, Mars. *Science* 360, 1096 LP – 1101.

Ferrage, E., Lanson, B., Sakharov, B.A., Drits, V.A. (2005) Investigation of smectite hydration properties by modeling experimental X-ray diffraction patterns: Part I. Montmorillonite hydration properties. *American Mineralogist* 90, 1358–1374.

Freissinet, C., Glavin, D.P., Mahaffy, P.R., Miller, K.E., Eigenbrode, J.L., Summons, R.E., Brunner, A.E., Buch, A., Szopa, C., Archer, P.D., Franz, H.B., Atreya, S.K., Brinckerhoff, W.B., Cabane, M., Coll, P., Conrad, P.G., Des Marais, D.J., Dworkin, J.P., Fairén, A.G., François, P., Grotzinger, J.P., Kashyap, S., Kate, I.L., Leshin, L.A., Malespin, C.A., Martin, M.G., Martin-Torres, F.J., McAdam, A.C., Ming, D.W., Navarro-González, R., Pavlov, A.A., Prats, B.D., Squyres, S.W., Steele, A., Stern, J.C., Sumner, D.Y., Sutter, B., Zorzano, M.-P. (2015) Organic molecules in the Sheepbed Mudstone, Gale Crater, Mars. *Journal of Geophysical Research: Planets* 120, 495–514.

Gautier, M., Muller, F., Le Forestier, L. (2017) Interactions of ammonium-smectite with volatile organic compounds from leachates. *Clay Minerals* 52, 143–158.

Grotzinger, J.P., Sumner, D.Y., Kah, L.C., Stack, K., Gupta, S., Edgar, L., Rubin, D., Lewis, K., Schieber, J., Mangold, N., Milliken, R., Conrad, P.G., DesMarais, D., Farmer, J., Siebach, K., Calef, F., Hurowitz, J., McLennan, S.M., Ming, D., Vaniman, D., Crisp, J., Vasavada, A., Edgett, K.S., Malin, M., Blake, D., Gellert, R., Mahaffy, P., Wiens, R.C., Maurice, S., Grant, J.A., Wilson, S., Anderson, R.C., Beegle, L., Arvidson, R., Hallet, B., Sletten, R.S., Rice, M., Bell, J., Griffes, J., Ehlmann, B., Anderson, R.B., Bristow, T.F., Dietrich, W.E., Dromart, G., Eigenbrode, J., Fraeman, A., Hardgrove, C., Herkenhoff, K., Jandura, L., Kocurek, G., Lee, S., Leshin, L.A., Leveille, R., Limonadi, D., Maki, J., McCloskey, S., Meyer, M., Minitti, M., Newsom, H., Oehler, D., Okon, A., Palucis, M., Parker, T., Rowland, S., Schmidt, M., Squyres, S., Steele, A., Stolper, E., Summons, R., Treiman, A., Williams, R., Yingst, A., Team, M.S.L.S. (2014) A Habitable Fluvio-Lacustrine Environment at Yellowknife Bay, Gale Crater, Mars. *Science* 343.

Kennedy, M.J., Pevear, D.R., Hill, R.J. (2002) Mineral Surface Control of Organic Carbon in Black Shale. *Science* 295, 657 LP – 660.

Kral, T.A., Birch, W., Lavender, L.E., Virden, B.T. (2014) Potential use of highly insoluble carbonates as carbon sources by methanogens in the subsurface of Mars. *Planetary and Space Science* 101, 181–185.

Laird, D.A., Scott, A.D., Fenton, T.E. (1989) Evaluation of the alkylammonium method of determining layer charge. *Clays and Clay Minerals* 37, 41–46.

Le Guillou, C., Bernard, S., De la Pena, F., Le Brech, Y. (2018) XANES-Based Quantification of Carbon Functional Group Concentrations. *Analytical Chemistry* 90, 8379–8386.

Marchi, S., Raponi, A., Prettyman, T.H., De Sanctis, M.C., Castillo-Rogez, J., Raymond, C.A., Ammannito, E., Bowling, T., Ciarniello, M., Kaplan, H., Palomba, E., Russell, C.T., Vinogradoff, V., Yamashita, N. (2019) An aqueously altered carbon-rich Ceres. *Nature Astronomy* 3, 140–145.

McMahon, S., Bosak, T., Grotzinger, J.P., Milliken, R.E., Summons, R.E., Daye, M., Newman, S.A., Fraeman, A., Williford, K.H., Briggs, D.E.G. (2018) A Field Guide to Finding Fossils on Mars. *Journal of Geophysical Research: Planets* 123, 1012–1040.

Mustard, J.F., M. Adler, A. Allwood, D.S. Bass, D.W. Beaty, J.F. Bell III, W.B. Brinckerhoff, M. Carr, D.J. Des Marais, B. Drake, K.S. Edgett, J. Eigenbrode, L.T. Elkins-Tanton, J.A. Grant, S. M. Milkovich, D. Ming, C. Moore, S. Murchie, T.C. Onstott, S.W, A.T. (2013) Report of the Mars 2020 Science Definition Team. Posted July, 2013, by the Mars Exploration Program Analysis Group (MEPAG) at *http://mepag.jpl.nasa.gov/reports/MEP/Mars_2020_SDT_Report_Final.pdf.*

Naimark, E., Kalinina, M., Shokurov, A., Boeva, N., Markov, A., Zaytseva, L. (2016) Decaying in different clays: implications for soft-tissue preservation. *Palaeontology* 59, 583–595.

Nordheim, T.A., Hand, K.P., Paranicas, C. (2018) Preservation of potential biosignatures in the shallow subsurface of Europa. *Nature Astronomy* 2, 673–679.

Osinski, G.R., Tornabene, L.L., Banerjee, N.R., Cockell, C.S., Flemming, R., Izawa, M.R.M., McCutcheon, J., Parnell, J., Preston, L.J., Pickersgill, A.E., Pontefract, A., Sapers, H.M., Southam, G. (2013) Impact-generated hydrothermal systems on Earth and Mars. *Icarus* 224, 347–363.

Sagemann, J., Bale, S.J., Briggs, D.E.G., Parkes, R.J. (1999) Controls on the formation of authigenic minerals in association with decaying organic matter: an experimental approach. *Geochimica et Cosmochimica Acta* 63, 1083–1095.

Saxby, J. (2012) The significance of organic matter in ore genesis. *Geochemical Studies* 2, 111.

Schwenzer, S.P., Kring, D.A. (2009) Impact-generated hydrothermal systems capable of forming phyllosilicates on Noachian Mars. *Geology* 37, 1091–1094.

Steele, A., McCubbin, F.M., Fries, M.D. (2016) The provenance, formation, and implications of reduced carbon phases in Martian meteorites. *Meteoritics & Planetary Science* 51, 2203–2225.

Steele, A., Benning, L.G., Wirth, R., Siljeström, S., Fries, M.D., Hauri, E., Conrad, P.G., Rogers, K., Eigenbrode, J., Schreiber, A., Needham, A., Wang, J.H., McCubbin, F.M., Kilcoyne, D., Rodriguez Blanco, J.D. (2018) Organic synthesis on Mars by electrochemical reduction of CO2. *Science Advances* 4, eaat5118.

Summons, R.E., Albrecht, P., McDonald, G., Moldowan, J.M. (2008) Molecular Biosignatures. In: Botta, O., Bada, J.L., Gomez-Elvira, J., Javaux, E., Selsis, F., Summons, R. (Eds) *Strategies of Life Detection*. Springer US, Boston, MA, 133–159.

Vago, J.L., Westall, F., Pasteur Instrument Teams and Other Contributors, L.S.S.W.G., Coates, A.J., Jaumann, R., Korablev, O., Ciarletti, V., Mitrofanov, I., Josset, J.-L., De Sanctis, M.C., Bibring, J.-P., Rull, F., Goesmann, F., Steininger, H., Goetz, W., Brinckerhoff, W., Szopa, C., Raulin, F., Westall, F., Edwards, H.G.M., Whyte, L.G., Fairén, A.G., Bibring, J.-P., Bridges, J., Hauber, E., Ori, G.G., Werner, S., Loizeau, D., Kuzmin, R.O., Williams, R.M.E., Flahaut, J., Forget, F., Vago, J.L., Rodionov, D., Korablev, O., Svedhem, H., Sefton-Nash, E., Kminek, G., Lorenzoni, L., Joudrier, L., Mikhailov, V., Zashchirinskiy, A., Alexashkin, S., Calantropio, F., Merlo, A., Poulakis, P., Witasse, O., Bayle, O., Bayón, S., Meierhenrich, U., Carter, J., García-Ruiz, J.M., Baglioni, P., Haldemann, A., Ball, A.J., Debus, A., Lindner, R., Haessig, F., Monteiro, D., Trautner, R., Voland, C., Rebeyre, P., Goulty, D., Didot, F., Durrant, S., Zekri, E., Koschny, D., Toni, A., Visentin, G., Zwick, M., van Winnendael, M., Azkarate, M., Carreau, C., Team, the E.P. (2017) Habitability on Early Mars and the Search for Biosignatures with the ExoMars Rover. *Astrobiology* 17, 471–510.

Viennet, J.-C., Bultel, B., Riu, L., Werner, S.C. (2017) Dioctahedral Phyllosilicates Versus Zeolites and Carbonates Versus Zeolites Competitions as Constraints to Understanding Early Mars Alteration Conditions. *Journal of Geophysical Research: Planets* 122.

Viennet, J.-C., Bultel, B., Werner, S.C. (2019) Experimental reproduction of the martian weathering profiles argues for a dense Noachian CO_2 atmosphere. *Chemical Geology* 525, 82–95.

Westall, F., Foucher, F., Bost, N., Bertrand, M., Loizeau, D., Vago, J.L., Kminek, G., Gaboyer, F., Campbell, K.A., Bréhéret, J.-G., Gautret, P., Cockell, C.S. (2015) Biosignatures on Mars: What, Where, and How? Implications for the Search for Martian Life. *Astrobiology* 15, 998–1029.

Wordsworth, R.D. (2016) The Climate of Early Mars. *Annual Review of Earth and Planetary Sciences* 44, 381–408.

Geochemical Perspectives Letters

Experimental clues for detecting biosignatures on Mars

J.-C. Viennet, S. Bernard, C. Le Guillou, P. Jacquemot, E. Balan, L. Delbes, B. Rigaud, T. Georgelin, M. Jaber

Supplementary Information

The Supplementary Information includes:

- Materials and Methods
- Supplementary Information References

Materials and Methods

Selected Materials

Pure powders of yeast RNA (Sigma-Aldrich) and Mg-smectites synthetised in the lab from a hydrogel of saponite ($Na_{0.4}(Mg_3)(Al_{0.4},Si_{3.60})O_{10}(F_{0.05},OH_{0.95})_2$) were used for the present experiments. The hydrogel was obtained by mixing pure water, hydrofluoric acid, sodium acetate, magnesium acetate tetrahydrate, aluminium acetate basic and silica aerosol. The hydrogel was mixed at room temperature for 3 hours at room temperature (~20 °C) and then introduced in a PTFE-lined stainless steel autoclave. The autoclave was heated at 220 °C for 3 days. After cooling down at room temperature, 5 Ca-saturation cycles were performed for a total duration of ~60 H. The Ca-saturated Mg-smectites were then washed in pure water by centrifugation and dried at 60 °C.

Experimental procedure

We conducted hydrothermal experiments in a 100 mL Parr Reactor © in closed system. For the present study, we experimentally submitted 300 mg of Mg-smectites mixed with 150 mg of RNA to hydrothermal conditions at 200°C in 15 mL of pure bi-distilled water in equilibrium with a CO_2 atmosphere for 7 days at water-vapour pressure (i.e. 15.5 bars at 200 °C). We conducted additional experiments under the same conditions with RNA in absence of Mg-smectites and with Mg-smectites in absence of RNA as controls. Each experiment was performed three times to ensure reproducibility. Experimental residues were washed in pure water five times and dried at 50 °C for ~12 hours.

Analytical measurements

Carbon and nitrogen elemental analysis

Total carbon and nitrogen content were determined using a Flash 2000 Thermo CHNSO elemental analyser operating at ISTeP (France). A mass of 2 to 3 mg of residue was combusted under oxygen/helium flux at 960 °C. N_2, CO_2 released by combustion were separated by a chromatography column and quantified using a thermal conductivity detector. Soil samples were used as standards giving uncertainties at 0.02 wt. % for N and 0.07 wt. % for C.

X-Ray Diffraction measurements

XRD patterns were obtained on a Panalytical X'pert Pro MPD 2 circles operating at IMPMC (Paris, France) at 20 °C and atmospheric pressure. The bulk XRD experiments were performed on powder. The scanning parameters for powder XRD under atmospheric pressure were 0.033°2θ for the step size and 250 s for the counting time per step throughout the 3–65°2θ CuK$\alpha_{1,2}$ angular range. The experiments dedicated to organic matter location were performed on oriented preparations at both atmospheric pressure and under vacuum (3.10^{-4} atmosphere) using an Anton Parr HTK 1200 oven and a temperature monitor TCU1000N coupled to an EDWARDS RV3 pump. The divergence slit, the anti-scatter slit and the two Soller slits were 0.5°, 1°, 0.04° and 0.04 radiant, respectively.

Mid-Infrared (MIR) spectroscopy

Fourier-tranform infrared (FT-IR) spectra have been recorded in the 400-4000 cm^{-1} range with a 4 cm^{-1} resolution using a Nicolet 6700 FTIR spectrometer fitted with a KBr beamsplitter and a DTGS-KBr detector. The powder spectra have been obtained under ambient conditions by averaging 200 scans obtained in attenuated total reflectance (ATR) geometry using a Specac Quest ATR device fitted with a diamond internal reflection element.

Sample preparation for STEM and STXM-XANES experiments

Cryo-ultramicrotome sections (70 nm thick) were prepared for STXM and TEM characterisation using the Leica ultramicrotome available at UMET (Lille, France). Experimental residues were mixed with 0.1 ml of water-ethanol (50/50 $\%_{Vol}$) before being frozen in liquid nitrogen at -160 °C. After cutting, the ultrathin slices of residues were deposited on holey carbon film TEM grids before being exposed to ambient temperature.

STXM-XANES measurements

XANES data were collected using a scanning transmission X-ray microscope on the HERMES STXM beamline (Belkhou *et al*., 2015; Hitchcock, 2018) at the synchrotron SOLEIL. Beamline optical elements were exposed to a continuous flow of pure O_2 to remove carbon contamination. Energy calibration was done before measurements using the well-resolved 3p Rydberg peak of gaseous CO_2 at 294.96 eV. XANES data were extracted from image stacks collected at energy increments of 0.1 eV over the carbon (270–350 eV) absorption range with a dwell time of ≤ 1 ms per pixel to prevent irradiation damage (Wang *et al*., 2009). Alignment of stack images and extraction of XANES spectra were done using the latest version aXis2000 software. The C-XANES spectra shown in the present contribution correspond to homogeneous carbon-rich areas of several hundreds of square nanometres and were normalised to the carbon quantity by integrating the spectra (after subtraction of a power law background) from the pre-edge region up to the mean ionization energy (*e.g*. 282-291.5 eV at the C K edge) following the method proposed and validated by Le Guillou *et al*., 2018).

TEM analyses and post-acquisition data processing

Scanning transmission electron microscopy (STEM) and EDS mapping were performed using a Thermofisher Titan Themis 300 microscope operated at 300 keV, located at the "centre commun de microscopie – CCM" at the university of Lille. Hyperspectral EDS data were obtained using the super-X detector system equipped with four windowless silicon drift detectors. These detectors have a high sensitivity for light elements and allow a high counting rate of the carbon, nitrogen and oxygen X-rays. The probe current was set at 600 pA with a dwell time at 10 µs per pixel.

A key aspect of this work is the post-processing of the hyperspectral data, performed using the Hyperspy python-based package (De La Peña *et al*., 2018). The signal was first denoised using PCA. Then, the EDS spectra at each pixel were fitted by a series of Gaussian functions and a physical model for background/bremsstrahlung. The integrated intensities of the Gaussian functions were used to quantify the compositions thanks to the Cliff-Lorimer method, using experimentally determined k-factors. Absorption correction was taken into account, which is mandatory to correct for the re-absorption within the sample of the carbon, nitrogen and oxygen X-rays. These steps correct for the thickness of the sample. Finally, end-member phases (smectites, phosphates, amorphous silicon oxides, organic compounds) were identified and their spectra used as inputs for linear combination fitting (multiple linear least square fits). Pixels of similar composition were given the same colors scaled as a function of the proportion of each phase.

Supplementary Information References

Belkhou, R., Stanescu, S., Swaraj, S., Besson, A., Ledoux, M., Hajlaoui, M., Dalle, D. (2015) HERMES: a soft X-ray beamline dedicated to X-ray microscopy. *Journal of Synchrotron Radiation* 22, 968–979.

De La Peña, F. de la, Fauske, V.T., Burdet, P., Prestat, E., Jokubauskas, P., Nord, M., Ostasevicius, T., MacArthur, K.E., Sarahan, M., Johnstone, D.N., Taillon, J., Eljarrat, A., Migunov, V., Caron, J., Furnival, T., Mazzucco, S., Aarholt, T., Walls, M., Slater, T., Winkler, F., Martineau, B., Donval, G., McLeod, R., Hoglund, E.R., Alxneit, I., Hjorth, I., Henninen, T., Zagonel, L.F., Garmannslund, A., Skorikov, A. (2018) hyperspy/hyperspy v1.4.1. doi: 10.5281/ZENODO.1469364

Hitchcock, A.P. (2018) aXis-2000 is an IDL-based analytical package 2000.

Le Guillou, C., Bernard, S., De la Pena, F., Le Brech, Y. (2018) XANES-Based Quantification of Carbon Functional Group Concentrations. *Analytical Chemistry* 90, 8379–8386. doi: 10.1021/acs.analchem.8b00689

Wang, J., Morin, C., Li, L., Scholl, A., Doran, A. (2009) Radiation damage in soft X-ray microscopy. *Journal of Electron Spectroscopy and Related Phenomena* 170, 25–36. doi: 10.1016/J.ELSPEC.2008.01.002